



Long-timescale fluctuations in zero-field magnetic vortex oscillations driven by dc spin-polarized current

V. S. Pribiag,¹ G. Finocchio,² B. J. Williams,³ D. C. Ralph,¹ and R. A. Buhrman¹

¹Cornell University, Ithaca, New York 14853, USA

²Dipartimento di Fisica della Materia ed Ingegneria Elettronica, University of Messina, Salita Sperone 31, 98166 Messina, Italy

³The University of Texas, Dallas, Texas 75080, USA

(Received 22 September 2009; published 12 November 2009)

We report time and frequency domain studies of spin-torque-driven vortex self-oscillations at zero magnetic field. We observe two types of abrupt fluctuations in the frequency and amplitude, with very long random mean lifetimes ($\sim 10^2$ to $\sim 10^4$ oscillation cycles). First, we observe fluctuations between two center frequencies separated by 10s of MHz that we identify with switching between quasiuniform and vortex states of the magnetic polarizing layer. Second, we resolve much smaller, discrete frequency fluctuations that lead to a fine structure of the oscillations. We find that this fine structure plays a key role in determining the long-time average linewidths and we suggest a possible physical origin.

DOI: [10.1103/PhysRevB.80.180411](https://doi.org/10.1103/PhysRevB.80.180411)

PACS number(s): 75.75.+a, 85.75.-d, 72.25.Ba, 72.25.Pn

The spin torque exerted by a spin-polarized current can excite a wide range of magnetization changes in magnetic nanostructures. Of special interest is the excitation of persistent GHz-frequency oscillations by dc currents. This autogeneration phenomenon has increased interest in magnetism-related nonlinear phenomena and is promising for potential on-chip, tunable dc-driven microwave sources. The majority of studies to date have focused on devices with strong in-plane magnetic anisotropy that oscillate in a quasiuniform (QU) spatial mode under applied field H of 100s to 1000s of Oe. Recently, studies have demonstrated that the spin torque can also excite persistent GHz oscillations in the absence of any applied magnetic field.¹⁻³ References 1 and 3 showed that by making use of the well-known precessional mode⁴⁻⁶ of a magnetic vortex (V) in a nanoscale point-contact or nanopillar structure, it is possible to obtain not only zero-field oscillations but also sub-MHz linewidths, considerably narrower than the 10s to 100s of MHz linewidths typically observed in the conventional vortex-free spin-torque oscillators. Spin-torque-driven vortex self-oscillations have since been observed by other experiments^{7,8} and have been the subject of theoretical studies aimed at better understanding the types of dynamics that can be excited by dc spin-polarized currents in nonuniform states,⁹ as well as the range of applicability for the equations of motion of magnetic vortices.¹⁰ An understanding of the factors affecting the stability of these oscillators and the sources of linewidth broadening are of great importance for further advances.

In this Rapid Communication, we report time-average and single-shot transport measurements and comparisons with micromagnetic simulations that reveal the existence of a mode substructure of the vortex self-oscillations. By simultaneously analyzing the oscillations in the frequency and time domains, we find that the substructure of the oscillations plays a key role in determining the average linewidth. The measurements are performed in $H=0$, as this is perhaps the most technologically important bias regime. The devices studied here are spin-valve nanopillars composed of $\text{Ni}_{81}\text{Fe}_{19}$ (60 nm)/Cu(40 nm)/ $\text{Ni}_{81}\text{Fe}_{19}$ (5 nm), with approximately elliptical cross sections (dimensions for each de-

vice are specified below) fabricated as described in Ref. 3. In equilibrium, the thick Py layer has a vortex configuration and the thinner polarizing layer a uniform in-plane magnetization, but as we discuss below, an alternative configuration is also possible at high bias currents.

The dependence of the frequency (f) and linewidth [full width at half maximum (FWHM)] on current (I) for one such device (dev. 1, nominal dimensions 80 nm \times 180 nm), as measured with a spectrum analyzer, are shown in Fig. 1. Although the vortex oscillations are expected to be single mode, corresponding to the gyrotropic precession of the core, the spectrum actually shows two different modes as a function of bias. The lower-frequency mode (M1) and the higher-frequency mode (M2) appear to coexist for I between ~ 6.5 and 9.5 mA. The presence of two modes at $H=0$ is a feature of all devices we studied, although the details of the bias dependence varied from sample to sample. For dev. 1, the two modes have an approximately linear dependence of frequency on current with average slopes of 3.3 MHz/mA for M1 and 6.5 MHz/mA for M2. The linewidths increase at a rate of 0.5 MHz/mA for M1 and ~ 1.0 MHz/mA for M2, but a stronger dependence is observed for M1 at small and large biases.

To obtain information about time correlations between the two modes, we have performed single-shot time-domain measurements. By band-pass filtering the time-domain signals we were able to reduce the noise background suffi-

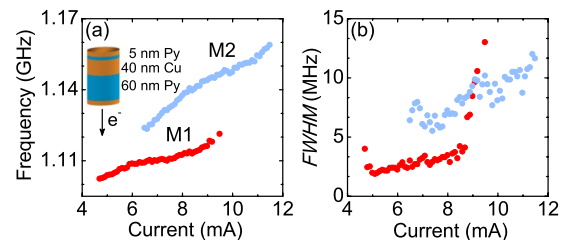


FIG. 1. (Color online) Current dependence of (a) frequency and (b) FWHM measured on dev. 1. (a) Inset: schematic of device geometry, showing the direction of electron flow under dc bias.

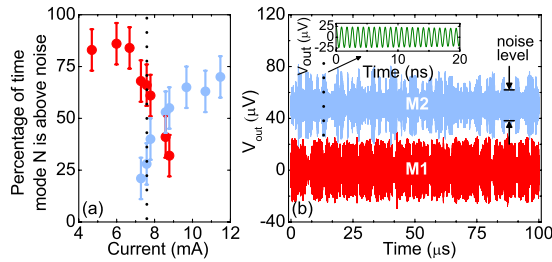


FIG. 2. (Color online) (a) Percentage of time spent oscillating above noise floor in modes M1 and M2 as a function of I , for dev. 1, obtained from a 100 μs time trace. (b) Digitally filtered time traces for modes M1 and M2 at 7.6 mA. V_{out} is the voltage delivered to the 50 Ω line. The time trace for M2 is offset by 50 μV for clarity. Inset: 20 ns subset of trace for M2.

ciently to study the time-dependent output of the devices. The digital filter bandwidth was adjusted for each peak as a function of its width (typical values were ~ 1.5 to 5 times the average linewidth) and was centered at the peak's main emission frequency. Figure 2 shows such time traces measured using a digital storage oscilloscope with an analog bandwidth of 3 GHz and sampling rate of 20 GS/s.

The time-domain measurements reveal that the system has only one major mode of oscillation at a given time but switches randomly between the two possible modes, with bias-dependent dwell times in the μs range. Figure 2(a) shows, as function of I , the fraction of time the system spends in each of the modes M1 and M2 for dev. 1. To obtain these data, we computed the envelope of 100 μs filtered traces, such as those shown in Fig. 2(b), and then determined the fraction of time the envelope was above the combined amplifier and Johnson noise floor. Mode M1 dominates from the onset of dynamics to ~ 6.0 mA, while M2 dominates for I larger than ~ 8.8 mA. A transition region is observed at intermediate biases.

The frequency shifts we report here are similar to the telegraph switching between spin-torque-excited dynamic modes previously observed in conventional spin valves,¹¹ but with the distinct difference that the timescales of the fluctuations in the case of the vortex oscillator are between two and three orders of magnitude longer than for the vortex-free spin valves. This indicates that the energy barrier retarding transitions between the two modes in the vortex oscillator system is much higher than for mode transitions in the quasiuniform spin-valve system or, alternatively, that the attractors that define the two modes in phase space for the vortex oscillator are much stronger than for quasiuniform spin valves.

To gain insight into the magnetic configurations associated with the experimental observations, we performed micromagnetic simulations¹² of the entire device, including the spin torque acting on both magnetic layers and the Oersted field due to the current.¹³ We simulated two device cross sections: an ideal ellipse and an additional cross section (shape A) modeled on a scanning electron microscope image of an actual device. Figure 3 shows the current dependence of the frequency and the linewidth extracted from Lorentzian fits to the fast Fourier transform (FFT) of the MR oscillations¹⁴ for the two shapes at a temperature (T) of 300

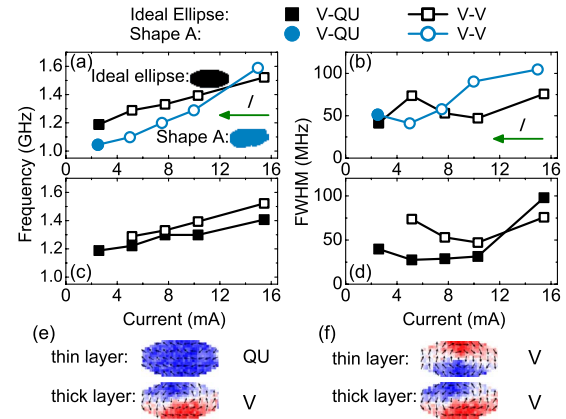


FIG. 3. (Color online) Simulated current dependence of (a) frequency and (b) FWHM, showing differences between two 75 nm \times 160 nm shapes, for decreasing I . Current dependence of (c) frequency and (d) FWHM for the ideal ellipse, showing difference between the V-QU and V-V configurations. (e) One of the two possible micromagnetic configurations, at 5.2 mA: V-QU. (f) The second possible configuration: V-V.

K and $H=0$. In the simulations, the current was initially set to a value of ~ 20 mA (ideal ellipse) and ~ 15 mA (shape A), then stepped down. The duration of the simulations, which was constrained by practical computation time length, limits the minimum linewidth to ~ 30 MHz. Due to the large initial current values, the devices start in a state with a vortex in the thin polarizing layer, in addition to the stable vortex in the thick layer. The chirality of the thick layer vortex is given by the Oersted field, while that of the thin layer vortex is opposite, due to the spin torque from the reflected spin polarization. At the initial large bias, the dynamics are highly chaotic and the frequency is not well defined. As the current is stepped down, the precession of the coupled pairs of vortices becomes regular and the oscillation linewidth narrows. Eventually, between 5.2 and 2.5 mA, the thin layer configuration switches from a V to a QU configuration [Figs. 3(a) and 3(b)], with details depending on the simulated device shape.

For the ideal ellipse, we have also performed simulations, where the direction of the current ramp was increasing [Figs. 3(c) and 3(d)]. In this case, the thin layer remains in the QU configuration for I up to a value between ~ 15.5 and 20.6 mA, then switches to a vortex. This reveals the existence of a broad bias range between ~ 5 and ~ 16 mA, within which both QU and V configurations of the thin layer are stable over the 100 ns length of all simulations. These two magnetic configurations are shown in Figs. 3(e) and 3(f). The frequency difference between the two simulated modes, corresponding to the two magnetic configurations of the thin layer, varies with bias between ~ 30 and ~ 120 MHz, while the experimental frequency splitting between modes M1 and M2 of device 1 ranges from ~ 15 to ~ 27 MHz, with the smaller difference perhaps being due to the nonideal shape of the experimental device. The simulated linewidth for the V-QU configuration is lower than for the V-V configuration at low currents and increases sharply at larger bias, in qualitative agreement with the experimental observation for dev. 1.

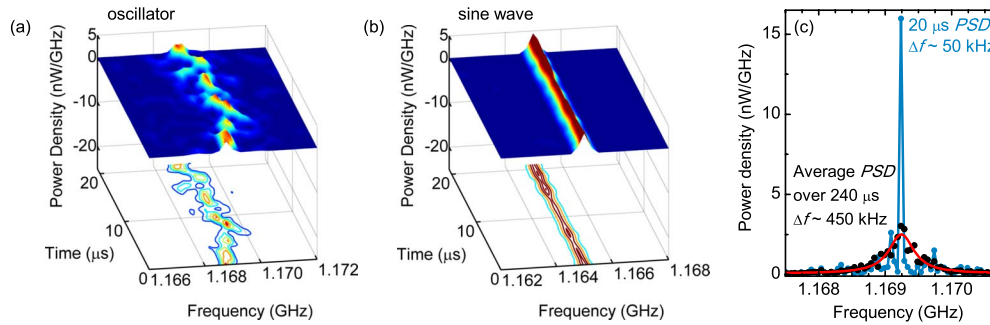


FIG. 4. (Color online) Spectrogram of (a) dev. 2 at $I=3.8$ mA, showing discrete frequency and amplitude fluctuations and (b) a 1.165 GHz sine wave with similar total power to device in (a), measured with the same circuit. The power fluctuations visible in (b) display the electronic noise added by the measurement circuit. (c) Average PSD of a 240 μs time trace from dev. 2 (black dots) and corresponding Lorentzian fit (red, lower line) with $\Delta f \sim 450$ kHz; PSD of a 20 μs contiguous subtrace (blue, upper line), with $\Delta f \sim 50$ kHz, limited by the length of the rectangular time window.

The good qualitative agreement of the simulations with the experiment suggests that the lower-frequency experimental mode M1 corresponds to the V-QU configuration, while M2 corresponds to the V-V configuration, with the data in Fig. 2(a) indicating that V-QU has the dominant lifetime at low bias and V-V is dominant at large bias. While the time-domain measurements show that modes M1 and M2 are metastable, their lifetimes are ≥ 1 μs , even when the bias is such that these dwell times are comparable. This is more than an order of magnitude longer than the duration of the simulations, which therefore do not capture the reversible jumps between V-V and V-QU seen experimentally.

Since the dwell times of the two modes, as determined by the time-domain measurements, are generally on the order of 1 μs to 10s of μs , except at the extremes of the bias range for oscillation, mode jumping due to abrupt changes in the overall magnetic configuration of the thin layer is not a dominant contribution to the individual mode linewidths, >1 MHz, obtained from time-averaged frequency measurements. Instead, we find by higher-resolution time-domain studies that each peak exhibits a substructure caused by abrupt small-scale changes in its frequency and amplitude, also with slow characteristic timescales of 100s of ns to μs . Figure 4(a) shows the Fourier spectrogram of a 5 GS/s time trace of mode M1 from a second device (dev. 2, 75 nm \times 155 nm) obtained by sliding a 4- μs -long Hann window¹⁵ across the time trace in 20 ns steps. The spectrogram of a sine wave with similar frequency and integrated power produced with a commercial generator, shown for comparison in Fig. 4(b), displays a stable frequency with the power clearly concentrated within the resolution bandwidth. In contrast, the device oscillations exhibit fluctuations of the frequency that are abrupt on the μs timescale of the measurement, as well as fluctuations in the shape and width of the spectrogram. These fluctuations qualitatively resemble those recently reported in vortex-free MgO magnetic tunnel junctions (MTJ) (Ref. 16); however, the timescales for our vortex spin valves are orders of magnitude longer than the ns timescales reported for the vortex-free MTJs, indicating that the vortex oscillations are much more coherent. Moreover, while Ref. 16 reports that discrete amplitude fluctuations dominate at low bias and continuous frequency fluctuations are dominant

at high bias for vortex-free MTJs, we find that for vortex spin valves the fluctuations can have a discrete character across the entire bias range we studied.

The small, discrete frequency jumps are particularly relevant since they appear to be the dominant contributor to the average linewidth of the vortex oscillator. In the intervals between these jumps, the linewidth can be quite narrow. For example, a typical long-time-averaged power spectral density (PSD) yields a relatively broad FWHM of 450 kHz, while the PSD of one of the 20 μs long intervals within this longer trace has a FWHM equal to the 50 kHz bandwidth set by the measurement window [Fig. 4(c)]. This ninefold reduction in the linewidth shows that the oscillator can be stable to better than 5×10^{-5} over 10s of μs (more than 10^4 cycles) before an abrupt change alters the center frequency. The corresponding value for the length of stable oscillations in vortex-free MTJs is just 10s of ns.¹⁶ The much slower timescales of the fluctuations for the vortex oscillator are another sign of its greater stability, in addition to its much narrower intrinsic linewidths (50 kHz min) compared to the vortex-free MTJs (~ 1 MHz min), albeit at the lower frequency of the vortex gyrotropic mode.

An analytical model of linewidth broadening in spin-torque oscillators has been proposed¹⁷ based on the effect of Gaussian thermal noise in a nonlinear system and has been found to be in good agreement with experiment for certain device geometries.¹⁸ Given the characteristics of thermal noise, the bandwidth of the resulting frequency fluctuations is expected to extend up to the ferromagnetic resonance frequencies of the magnetic elements within the device. This does not appear to be compatible with the dominant frequencies of the discrete fluctuations we observe in the vortex oscillator, which are two to three orders of magnitude slower.

We propose instead that these discrete μs -timescale frequency fluctuations result from abrupt changes in the non-ideal vortex orbit. The ability of static magnetic imperfections to affect vortex dynamics has been demonstrated by optical Kerr microscopy studies that have shown that the gyrotropic frequency of a vortex in a microscale thin-film structure can vary by a factor of 3 or more when the core is displaced relative to different pinning inhomogeneities.¹⁹ Due to the relatively small region covered by the precessing

core and the stronger confining potential in our nanopillars, we do not expect, nor observe, such large variations in the frequency. However, if the confining potential for the vortex is not ideal then abrupt changes in the orbit can occur if, on the same timescale, there are either abrupt changes in the magnetic configuration that defines that potential, which could be due to thermal or spin-torque excitations, or if there are chaotic transitions between different attractors in the non-ideal phase space.²⁰ According to the simulations, which assume a magnetically perfect, albeit digitally modeled system, the vortex oscillator can indeed be chaotic, even at $T=0$, due in part to the spin-torque excitation of localized magnetic dynamics. Although direct comparison with experiment is impossible due to the short simulation times, the fact that at sufficiently high bias, both in the experiment and in the simulations, the vortex oscillator linewidth broadens and the device behavior becomes chaotic, with the oscillation eventually breaking down, suggests that spin-torque excitation of localized magnetic dynamics could be a significant contribution to the smaller-scale linewidth broadening observed by the time-domain measurements at moderate bias levels.

In conclusion, our results show that zero-field spin-torque-driven vortex self-oscillations are characterized by very long timescale fluctuations (100s of ns to 10s of μ s). By means of single-shot time-domain measurements, we can re-

solve two main types of fluctuations. The first are due to transitions of the thin polarizing magnetic layer between quasiuniform and vortex configurations, resulting in shifts of 10s of MHz in the ~ 1 GHz vortex gyrotropic frequency. The second are smaller fluctuations that appear to be the dominant contribution to the long-time average linewidth of the vortex oscillator. The discrete, low-frequency character of these smaller fluctuations suggests that the dominant linewidth broadening mechanisms are either dynamic changes in the magnetic configuration that defines the vortex orbit or chaotic transitions between attractors in the phase space established by the device shape and defect configuration. A stronger confining potential would reduce the sensitivity of the orbit to magnetic defects and hence could better stabilize it. The use of smaller devices and more homogeneous thin films could therefore yield significant improvements in vortex oscillator properties.

We thank B. Azzarboni, P. Brouwer, and L. Torres for discussions and N. Civiletti for assistance with simulations. This research was supported in part by the Office of Naval Research, the Army Research Office, and the NSF through its NSEC program and was performed in part at the Cornell NanoScale Facility, which is supported by the NSF.

¹M. R. Pufall, W. H. Rippard, M. L. Schneider, and S. E. Russek, *Phys. Rev. B* **75**, 140404(R) (2007).

²O. Boulle, V. Cros, J. Grollier, L. G. Pereira, C. Deranlot, F. Petroff, G. Faini, J. Barnas, and A. Fert, *Nat. Phys.* **3**, 492 (2007).

³V. S. Pribiag, I. N. Krivorotov, G. D. Fuchs, P. M. Braganca, O. Ozatay, J. C. Sankey, D. C. Ralph, and R. A. Buhrman, *Nat. Phys.* **3**, 498 (2007).

⁴K. Y. Guslienko, B. A. Ivanov, V. Novosad, Y. Otani, H. Shima, and K. Fukamichi, *J. Appl. Phys.* **91**, 8037 (2002).

⁵J. P. Park, P. Eames, D. M. Engebretson, J. Berezovsky, and P. A. Crowell, *Phys. Rev. B* **67**, 020403(R) (2003).

⁶V. Novosad, F. Y. Fradin, P. E. Roy, K. S. Buchanan, K. Y. Guslienko, and S. D. Bader, *Phys. Rev. B* **72**, 024455 (2005).

⁷Q. Mistral, M. van Kampen, G. Hrkac, J.-V. Kim, T. Devolder, P. Crozat, C. Chappert, L. Lagae, and T. Schrefl, *Phys. Rev. Lett.* **100**, 257201 (2008).

⁸R. Lehdorff, D. E. Bürgler, S. Gliga, R. Hertel, P. Grünberg, C. M. Schneider, and Z. Celinski, *Phys. Rev. B* **80**, 054412 (2009).

⁹B. A. Ivanov and C. E. Zaspel, *Phys. Rev. Lett.* **99**, 247208 (2007).

¹⁰A. V. Khvalkovskiy, J. Grollier, A. Dussaux, K. A. Zvezdin, and V. Cros, *Phys. Rev. B* **80**, 140401(R) (2009).

¹¹I. N. Krivorotov, N. C. Emley, R. A. Buhrman, and D. C. Ralph, *Phys. Rev. B* **77**, 054440 (2008).

¹²G. Finocchio, I. N. Krivorotov, L. Torres, R. A. Buhrman, D. C. Ralph, and B. Azzarboni, *Phys. Rev. B* **76**, 174408 (2007); G. Siracusano, G. Finocchio, I. N. Krivorotov, L. Torres, G. Consolo, and B. Azzarboni, *J. Appl. Phys.* **105**, 07D107 (2009).

¹³The materials parameters are typical of Permalloy: saturation magnetization $M_s=650$ e.m.u/cm³, damping parameter $\alpha=0.01$, exchange constant $A=1.3$ μ erg/cm, and spin polarization $P=0.38$. $5 \times 5 \times 5$ nm³ cells were used.

¹⁴The frequency spectrum was computed by summing the absolute values of the FFTs of the MR time traces over all ballistic channels. A cosine angular dependence was used to compute the MR trace for each channel.

¹⁵W. W. Smith and J. M. Smith, *Handbook of Real-Time Fast Fourier Transforms* (IEEE Press, Piscataway, 1995).

¹⁶D. Houssameddine, U. Ebels, B. Dieny, K. Garello, J.-P. Michel, B. Delaet, B. Viala, M.-C. Cyrille, J. A. Katine, and D. Mauri, *Phys. Rev. Lett.* **102**, 257202 (2009).

¹⁷A. Slavin and V. Tiberkevich, *IEEE Trans. Magn.* **45**, 1875 (2009).

¹⁸C. Boone, J. A. Katine, J. R. Childress, J. Zhu, X. Cheng, and I. N. Krivorotov, *Phys. Rev. B* **79**, 140404(R) (2009).

¹⁹R. L. Compton and P. A. Crowell, *Phys. Rev. Lett.* **97**, 137202 (2006).

²⁰K.-J. Lee, A. Deac, O. Redon, J.-P. Nozieres, and B. Dieny, *Nature Mater.* **3**, 877 (2004).